ISSN 0001-4370, Oceanology, 2025, Vol. 65, No. 4, pp. 481–499. © Pleiades Publishing, Inc., 2025.

MARINE PHYSICS

Behavior Modes of a Quasi-Geostrophic Ellipsoidal Vortex in a Horizontal Flow with Vertical Shear

D. A. Harutyunyan[a, *] and V. V. Zhmur[a, b]

[a] *Moscow Institute of Physics and Technology (National Research University), Dolgoprudny, Moscow oblast, 141701 Russia*

[b] *Shirshov Institute of Oceanology, Russian Academy of Sciences, Moscow, 117218 Russia*

**e-mail: arutyunyan.da@phystech.su*

Received December 18, 2024; revised January 14, 2025; accepted January 26, 2025

Abstract—This paper addresses the problem of behavior modes of baroclinic geostrophic vortices with ellipsoid-shaped cores in horizontal flows with vertical shear. In such flows, a vortex core is confined between two stationary horizontal planes that the vortex contacts with its upper and lower points. Under the background flow effect, the length of all ellipsoid axes can change in space, as do vortex orientation angles. We identify three vortex behavior modes. The first mode is vortex survival in a shear flow where the vortex undergoes finite oscillations of its semi-axes for an indefinite period of time and can exhibit complicated behavior in terms of its orientation angles. This mode corresponds to strong vortices. In the second mode, the vortex elongates along the flow from the beginning, remaining with finite horizontal dimensions perpendicular to the flow, and is compressed vertically. This mode involves the destruction of the vortex by the flow, resulting finally in a thin vertical ocean structure formed from the vortex. Weak vortices undergo this type of evolution. This type is referred to as the "unlimited elongation mode." Finally, the third mode is called the "finite lifetime mode": for a finite period of time, the vortex behaves similarly to the survival mode (its shape is deformed in a finite manner and it rotates or oscillates in space), but eventually the vortex elongates indefinitely in a manner similar to the destruction mode. We outline the region of each mode on a dimensionless parameter plane of the problem and define the boundaries between the above-mentioned vortex behavior modes.

Keywords: ellipsoidal vortex, vortex core, baroclinic flow, vertical shear, finite vortex lifetime mode, and elongation mode

DOI: 10.1134/S000143702570016X

INTRODUCTION

Mesoscale ocean variability became relevant for study after an anticyclonic vortex was discovered in the North Atlantic region in 1970 during the POLYGON-70 expedition. This vortex was elliptical in shape with 90 and 180 km semi-axes, slowly rotating as a whole, while simultaneously moving westward at 2 cm/s with a small southern component of about 1 cm/s. The orbital velocity of its particles was maximum at a depth of 400–600 m. In the course of the POLYGON-70 expedition the internal radius of the Rossby deformation L_R was about ~65 km. This value makes it possible to confidently state that this vortex is related to mesoscale ocean phenomena. Subsequently, well-known marine experiments such as MODE (Sargasso Sea, 1973), POLIMODE (North Atlantic region, 1977–1978), MESOPOLYGON (North Atlantic region, 1985), MEGAPOLIGON (Pacific Ocean, 1987), etc. were conducted to study the vortex trends in the oceans. It became clear that vortices made a considerable contribution to the transport of salt, heat, and different impurities, were actively involved in the mixing of ocean waters, and ultimately substantially affected the changing climate. As a result, the demand for research into theoretical problems of geophysical hydrodynamics increased and the works on laboratory and numerical modeling of mesoscale ocean processes expanded.

The theoretical study of vortex behavior in flows began to be interesting for researchers as early as the beginning of the 20th century. Kirchhoff obtained an exact solution to the evolution of an equal-vortex elliptical region in 2D hydrodynamics of a perfect fluid in an infinity-based medium [8, 15]. The behavior of the Kirchhoff vortex in a shear flow was studied by Chaplygin [10, 12], but complete understanding of the evolution modes of the Kirchhoff vortex in equal-vortex flows was provided by the Japanese researcher Kida [14]. Kida's work served as an impetus for the study of vortices in plane hydrodynamics. In particular, Polvani and Flierl [20] developed a theory that generalized the Kirchhoff vortex. The theory of volumetric ellipsoidal vortices in the quasi-geostrophic approximation was developed in the 1990s [5, 19, 21]. The first works were focused on vortices with one vertical and two horizontal axes in barotropic equal-vortex flows of the Kida flow type. It turned out that the

behaviors of Kirchhoff elliptical vortices and indicated volumetric ellipsoidal vortices in equal-vortex barotropic flows were qualitatively very similar. Both have only three behavior modes of vortex cores: rotation or oscillation of shape around a vertical axis with simultaneous limited variation in the length of horizontal semi-axes and a mode of unlimited elongation of the vortex core in a horizontal plane. In the first two cases, the shape motion is periodic, while in the last case, it is aperiodic. The authors interpreted the unlimited elongation mode as a vortex destruction by flows.

Despite the fact that three vortex behavior modes in barotropic flows were established in the 1990s, quantitative criteria of different modes were obtained only in 2023 [2, 4]. The behavior of ellipsoidal vortices with arbitrary orientation in space and in more complex equal-vortex flows was studied in the 1990s in [6, 19]. These studies and generalizations were continued by the Dritschel school [13, 16–18] and by other authors. In addition, the study of finite-volume vortices was carried out in laboratory and natural conditions (for example, [1, 7]). Three Euler's angles or Cardan's angles were used to describe and change orientation angles of the ellipsoidal vortex core in space already in the first works [6, 19]. As a result, a relatively complicated system of six ordinary differential equations was obtained; it described the evolution of these angles and variations in a length of semi-axes of the ellipsoidal vortex core over time. However, a complete quantitative study of the core deformation behavior modes has not been carried out to date due to the complexity and multidimensionality of the system. Qualitative features of the solutions were considered to include the complicated behavior of vortex orientation in space and the emergence of new unlimited elongation modes under which, at the beginning, over a certain time interval the vortex underwent limited quasi-periodic oscillations of a length of semi-axes of the vortex core with a complicated behavior of orientation angles; the core was then almost stopped in space and elongated indefinitely by a background flow. This behavior was interpreted by the authors as vortex evolution in flows with a finite lifetime. For very closed conditions, the authors proposed the interpolation dependence of the lifetime on the vortex intensity and background flow shear. This work did not propose any other type of vortex behavior. When comparing the vortex behavior in barotropic and baroclinic flows in the above-mentioned works, we should note that no analogs of the vortex rotation and oscillation modes in barotropic flows for baroclinic flows were found; the unlimited vortex elongation mode became more complicated for baroclinic flows. Along with this, the above-mentioned works did not propose any quantitative criteria. As a result, a number of questions arise: (1) what vortex behavior modes exist in baroclinic flows? (2) is there a periodic or quasi-periodic behavior mode of the vortex parameters during its evolution in baroclinic flows?, and (3) if there are several modes, what quantitative criteria distinguish modes from each other? The background flow is considered to be horizontal flow with vertical shear. This is an example of the simplest equal-vortex baroclinic flow.

THE MATHEMATICAL STATEMENT OF THE PROBLEM

Based on [5, 6, 19], we consider a stratified rotating ocean with small Rossby numbers in the quasi-geostrophic approach $\mathrm{Ro} = \dfrac{U}{fL} \ll 1$ (U is the characteristic velocity of the process under study, L is the characteristic horizontal size, and $f = \mathrm{const}$ is the Coriolis parameter) in the f-plane approximation. In this case, the geophysical hydrodynamics equations are reduced to one equation for pressure or, in an equivalent formulation, to the flow function $\psi(x, y, z, t)$:

$$\frac{\partial}{\partial t}\left(\Delta_h\psi + \frac{\partial}{\partial z}\frac{f^2}{N^2}\frac{\partial\psi}{\partial z}\right) + J_h\left(\psi, \Delta_h\psi + \frac{\partial}{\partial z}\frac{f^2}{N^2}\frac{\partial\psi}{\partial z}\right) = 0, \quad (1)$$

where x and y are fixed horizontal axes of the coordinate system; z is the vertical axis; $J_h(A, B) = \dfrac{\partial A}{\partial x}\dfrac{\partial B}{\partial y} - \dfrac{\partial A}{\partial y}\dfrac{\partial B}{\partial x}$ is the Jacobi determinant (Jacobian); $\Delta_h = \dfrac{\partial^2}{\partial x^2} + \dfrac{\partial^2}{\partial y^2}$ is the Laplace operator in horizontal coordinates; and $N(z)$ is the Vaisala–Brunt frequency.

If the flow function $\psi(x, y, z, t)$ is calculated, then all other hydrodynamic characteristics of the motion can be determined, for example, the velocity field (u, v, w):

$$u = -\frac{\partial\psi}{\partial y}, \quad v = \frac{\partial\psi}{\partial x}, \quad w = -\frac{f_0}{N^2}\left[\frac{\partial^2\psi}{\partial t\partial z} + J_h\left(\psi, \frac{\partial\psi}{\partial z}\right)\right]. \quad (2)$$

In this case, Eq. (1) takes only the geostrophic part of the horizontal motion into account, as evidenced by the first two relations (2). The non-geostrophic component of the velocity in terms of this formulation is small (about $O(\mathrm{Ro})$) and cannot be obtained from approximation (1).

Equation (1) states that

$$\sigma = \Delta_h\psi + \frac{\partial}{\partial z}\frac{f^2}{N^2}\frac{\partial\psi}{\partial z} \quad (3)$$

with the same accuracy of about $O(\mathrm{Ro})$ is the Lagrangian invariant and is transferred together with a moving fluid particle. The preserved value σ is called

the potential vorticity or a potential vortex. This name was introduced by Rossby, and relation (3) will therefore occasionally be called the "potential vorticity according to Rossby." It should be noted that $\Delta_h\psi = \mathrm{rot}_z\vec{u}$. The potential vorticity σ is formed by the relative vorticity $\mathrm{rot}_z\vec{u}$ and vertical compression–elongation of a liquid particle (term $\frac{\partial}{\partial z}\frac{f^2}{N^2}\frac{\partial\psi}{\partial z}$). If $N = \mathrm{const}$, relation (3) can be simplified. In fact, if the concept of "elongated" vertical coordinate $\tilde{z} = \frac{N}{f}$ is introduced, then the $\frac{\partial}{\partial z}\frac{f^2}{N^2}\frac{\partial}{\partial z}$ operator can be written as $\frac{\partial}{\partial z}\frac{f^2}{N^2}\frac{\partial}{\partial z} = \frac{\partial^2}{\partial\tilde{z}^2}$, and relation (3) can be represented as a 3D Laplace operator $\Delta = \frac{\partial^2}{\partial x^2} + \frac{\partial^2}{\partial y^2} + \frac{\partial^2}{\partial\tilde{z}^2}$ in the vertically "elongated" space $(x, y, \tilde{z})$:

$$\sigma = \Delta_h\psi + \frac{\partial^2\psi}{\partial\tilde{z}^2} = \Delta\psi. \tag{4}$$

Relation (4) can be interpreted as the distribution of potential vorticity σ in "elongated" space. This approach is especially efficient for piecewise constant distributions. For example, it is assumed that the potential vorticity of particles is constant $\sigma_{\text{in}} = \text{const}$ in some closed volume V of space $(x, y, \tilde{z})$, and outside this volume, the potential vorticity is also constant, but it is already a different constant $\sigma_{\text{out}} = \text{const}$. The boundaries of region V are mobile and deformable. The deformable volume V is called "a vortex core" or "a vortex's core." Particles occurred inside the region V move along with it. The difference in the potential vorticity of particles inside and outside the vortex core is designated as $\sigma = \sigma_{\text{in}} - \sigma_{\text{out}}$. In terms of mathematics, the potential vorticity distribution in space can be written as

$$\Delta\psi = \begin{cases}\sigma_{\text{in}}, & \text{if } (x, y, \tilde{z}) \in V\\ \sigma_{\text{out}}, & \text{if } (x, y, \tilde{z}) \notin V.\end{cases} \tag{5}$$

The time t is included in (5) in terms of parameters and describes the deformation of V.

The hydrophysical interpretation of (5) is as follows. An ocean vortex consists of a vortex core with an increased vorticity and a surrounding fluid captured in motion. The vortex core is the above-mentioned volume V that carries rotating waters occurred inside the core. The fluid external to the core, which is involved in the circulation around the core, washes it and has a different vorticity compared to it, but is an integral part of the vortex formation. The evolution of the entire vortex is largely based on the vortex core behavior.

Due to the linearity of (5), this problem can be divided into two conditionally independent components: the background flow ψ_f with the equation valid in the entire space

$$\Delta\psi_f = \sigma_{\text{out}}, \tag{6}$$

and the disturbance of the background flow ψ_v by a vortex with the following potential vorticity distribution:

$$\Delta\psi_v = \begin{cases}\sigma, & \text{if } (x, y, \tilde{z}) \in V\\ 0, & \text{if } (x, y, \tilde{z}) \notin V.\end{cases} \tag{7}$$

As noted earlier, σ is the excess of potential vorticity of the vortex core σ_{in} over its background value σ_{out}. The background flow ψ_f is selected according to equation (6), while the vortex disturbance problem (7) should be solved separately.

Relation (7) is completely consistent with the problem of determining the gravity potential of a body with uniform density. In this case, the deformation of V is allowed. The solution to (7) can be given in general form for any V configuration. We are interested in the case when the shape of V is ellipsoid with principal directions (x_1, y_1, z_1) and values of the corresponding semi-axes (a, b, c). The solution to this problem is given below:

$$\psi_v(x_1, y_1, z_1, t) = -\frac{1}{4}\sigma abc\int_\lambda^\infty\left(1 - \frac{x_1^2}{a^2+\mu} - \frac{y_1^2}{b^2+\mu} - \frac{z_1^2}{c^2+\mu}\right) \times \frac{d\mu}{\sqrt{(a^2+\mu)(b^2+\mu)(c^2+\mu)}}. \tag{8}$$

In this case, the time t is included in (8) as a parameter meaning that the semi-axes (a, b, c), as well as directions of the principal axes, can depend on time as a parameter. The lower limit in the integral (8) $\lambda > 0$ is the positive root of the cubic equation

$$\frac{x_1^2}{a^2+\lambda} + \frac{y_1^2}{b^2+\lambda} + \frac{z_1^2}{\tilde{c}^2+\lambda} = 1. \tag{9}$$

The surface $\lambda = \text{const}$ corresponds to a confocal ellipsoid to the original ellipsoid under consideration. It is obvious that $\lambda > 0$ for external points (x_1, y_1, z_1). If the point (x_1, y_1, z_1) occurs inside the ellipsoid with semi-axes (a, b, c), then it is necessary to set $\lambda = 0$ for internal regions in (8).

Based on gravity potential theory [9], the function ψ and its first spatial derivatives are continuous. In our case, this is equivalent to the statement that a pressure field and a geostrophic velocity field are continuous. This remains valid for any deformation of V and arbitrary semi-axes–time relation. In turn, the pressure continuity means that the dynamic pressure equality condition on both sides of the boundary of the vortex's core is obviously met for solution (8) at the core's boundary. The kinematic condition at the same boundary is not yet met.

If the equation of the vortex core's boundary is designated as $F(x, y, \tilde{z}, t) = 0$ in a fixed coordinate system with horizontal axes (x, y), then the exact kinematic condition at this boundary is:

$$\frac{\partial F}{\partial t} + u\frac{\partial F}{\partial x} + v\frac{\partial F}{\partial y} + w\frac{\partial F}{\partial z} = 0. \quad (10)$$

In this case, the last term of Eq. (10) is small compared to similar terms of horizontal transfer $O\left(\frac{w\frac{\partial F}{\partial z}}{u\frac{\partial F}{\partial x}}\right) \sim \mathrm{R_O}$. Therefore, if we require the same accuracy for (10) as for the main Eq. (1), then the kinematic boundary condition (10) should be simplified:

$$\frac{\partial F}{\partial t} + u\frac{\partial F}{\partial x} + v\frac{\partial F}{\partial y} = 0. \quad (11)$$

In this relation, u and v are horizontal geostrophic flow velocities induced by the vortex plus external (background) geostrophic flows being the solution to problem (6). This approach implies the use of only equal-vortex flows as background flows, because they leave the core under deformation as an ellipsoid. In particular, the horizontal flow with vertical shear is considered as a candidate for this background flow:

$$\vec{u} = (\Gamma z, 0, 0), \quad (12)$$

It should be noted that solution (6) for an ellipsoidal shape of the core is written in a different (x_1, y_1, z_1) coordinate system where, in the general case, the axes are rotated relative to the fixed $(x, y, \tilde{z})$ coordinate system.

Neglecting the vertical velocity component in the boundary condition (11) leads to some important features. First, the vortex core during its evolution is confined between two stationary horizontal planes and contacts them with its upper and lower points. These points slide along the specified surfaces, preventing the core from rising above or falling below its location layer. The liquid vortex core "flows" and "turns inside out" inside the specified layer. Second, the cross-sectional area of the core with any horizontal plane is preserved during the core transformation. These features were noted in [6, 19].

The equation of the ellipsoidal surface of the vortex core is most simply written in the accompanying (x_1, y_1, z_1) coordinate system:

$$F(x_1, y_1, z_1, t) = \frac{x_1^2}{a^2} + \frac{y_1^2}{b^2} + \frac{z_1^2}{\tilde{c}^2} - 1 = 0. \quad (13)$$

The shape of this core depends on time t in terms of parameters through the time-varying semi-axes $a, b, \tilde{c}$ and the orientation of the coordinate axes (x_1, y_1, z_1). It should be noted that due to their large horizontal size compared to the vertical size of the vortex core, two semi-axes will be located almost horizontally in the real ocean conditions. These are designated as a and b. In this case, the third semi-axis $\tilde{c}$ will be almost vertical. Further, the indicated semi-axes a and b will be conditionally horizontal and the semi-axis $\tilde{c}$ will be conditionally vertical. The (x_1Oy_1) plane formed by the semi-axes a and b should be slightly inclined to the horizontal plane. The condition of gentle slopes can be violated for vortices with a small horizontal size, as observed in the Arctic Ocean seas where the internal radius of Rossby deformation is very low (about 5 km) and accordingly, the horizontal size of mesoscale vortices can also be small. This feature will not affect the mathematical terms of the matter; therefore, even in the case of noticeable deviations of the (x_1Oy_1) plane from the horizontal, we still call the semi-axes a and b "conditionally horizontal." The section of the core with the (x_1Oy_1) plane is called the main section of the vortex core.

The indicated relation (8) is an exact solution of the nonlinear Eq. (1) with nonlinear boundary conditions (11), which makes this solution a convenient reference point in solving similar problems, in particular, in the numerical study of sea movements under conditions close to quasi-geostrophic force equilibrium of forces, studies of the accuracy of difference schemes, etc.

The problem of the ellipsoidal vortex behavior in a horizontal flow with vertical shear (12) was partially covered in [6, 19]. However, these publications were not aimed at determining all vortex behavior modes in baroclinic flows with vertical shear (12). Nevertheless, the indicated works made it possible to derive differential equations describing the time-related behavior of a length of the semi-axes of the vortex ellipsoid and its three space orientation angles. We will take these works into consideration below.

THE MATHEMATICAL MODEL OF THE VORTEX BEHAVIOR IN A FLOW WITH VERTICAL SHEAR

It is convenient to work with dimensionless geometric parameters of the vortex to study its evolution. As such, we consider two dimensionless numbers. The first number is the ratio of conditional horizontal semi-axes of the vortex core $\varepsilon = \frac{a}{b}$. The parameter ε describes the vortex core deformation in the (x_1Oy_1) plane. By analogy with [5], we call ε "the elongation parameter" (almost horizontal elongation) of the vortex. Another dimensionless parameter $K = \frac{\tilde{c}}{\sqrt{ab}}$ represents relative flattening of the vortex toward the semi-axis $\tilde{c}$ and describes its relative thickness along the z_1 axis.

The Euler angles φ, Θ, and ψ are used to describe the vortex orientation in space. Figure 1 shows the range of successive core rotations at Euler angles.

A series of three rotations is carried out to obtain a current orientation of the vortex core from the initial position (X, Y, Z system): (1) rotation around the axis Z at the angle φ, at which the axes X and Y are transformed into X' and Y'; (2) rotation around the Y' axis

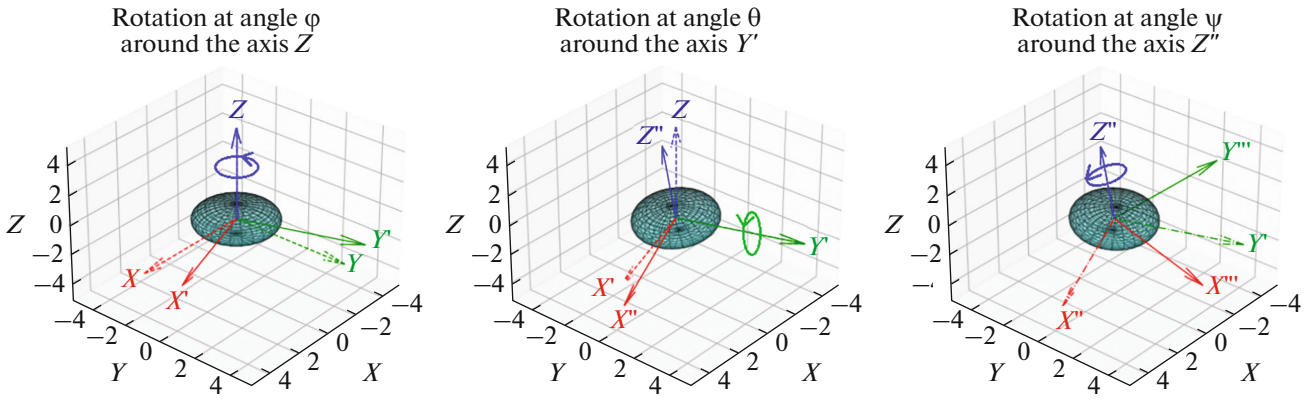

Fig. 1. The successive rotation of the core at Euler angles.

at angle Θ, at which the X' and Z axes are transformed into X' and Z'; and (3) rotation around the Z'' axis at the angle ψ, at which the X'' and Y' axes are transformed into X''' and Y'''. Hence, the vortex core geometry is completely based on three dimensional parameters $a, b, \tilde{c}$ and three dimensionless parameters φ, Θ, ψ. It should be noted that the vortex as a whole moves at a velocity of the background flow at the vortex center. Since we are interested only in the evolution of the vortex core boundary, rather than in its motion as a whole, we place the vortex center at the point (0, 0, 0), where the background flow velocity is zero. As a result, such vortex as a whole remains still, whereas its boundary can be deformed, and semi-axes and orientation angles can change.

The earlier solution (8) together with the background flow (12) meet Eq. (1). The pressure continuity (dynamic condition) pressure is automatically satisfied at the core's boundary, which is a jump in potential vorticity. Meanwhile, the kinematic condition (11) is not yet met for the given solution. This condition will make it possible to describe the evolution of geometric parameters of the vortex core.

The above-mentioned kinematic condition (11) is considered to estimate the vortex behavior in the background flow. It can be written in the following form [2, 6, 19]:

$$\nabla F \cdot (\vec{U} - \vec{V}) = 0, \tag{14}$$

where $\vec{V}$ is the core boundary velocity, $\vec{U}$ is the fluid particle velocity which consists of a vortex-induced flow velocity and the external flow velocity. Condition (14) can be conveniently represented in the (x_1, y_1, z_1) coordinate system related to the ellipsoid. In this case, the vertical component of the velocity in the fixed $(x, y, \tilde{z})$ system in Eq. (14) should not be taken into account, according to (11).

The use of the kinematic boundary condition (14) to obtain the equations for the evolution of vortex characteristics $a(t), b(t), \tilde{c}(t), \varphi(t), \Theta(t)$, and $\psi(t)$ was considered in detail in [6, 19] and repeated in [2]. Therefore, in this paper, we briefly outline the idea of deriving the equations for trends of the characteristics of the vortex; as for a detailed review, refer to the original sources [6, 19] or [2]. Further, for simplicity purposes, the value of the semi-axis $\tilde{c}(t)$ is designated as $c(t)$.

Condition (14) can also be written as a matrix:

$$\vec{x}_1^{\top} F (G + T - J - D) \vec{x}_1 = 0, \tag{15}$$

where F is determined from the ellipsoid surface Eq. (13) as

$$F = \begin{pmatrix} 1/a^2 & 0 & 0 \\ 0 & 1/b^2 & 0 \\ 0 & 0 & 1/c^2 \end{pmatrix}.$$

The $(G + T - J - D)\vec{x}_1$ matrix indicates velocity projection onto the axes of the accompanying (x_1, y_1, z_1) coordinate system. Each of these matrices is considered separately. The $G = R^{-1}SRP$ matrix describes the velocity of the fluid particle generated by the vortex, as obtained using the geostrophic relation in (2), where $S = \begin{pmatrix} 0 & -1 & 0 \\ 1 & 0 & 0 \\ 0 & 0 & 0 \end{pmatrix}$, R is the Euler angle rotation matrix:

$$R = \begin{pmatrix} -\sin\psi\sin\psi + \cos\theta\cos\varphi\cos\psi & -\sin\varphi\cos\psi - \sin\psi\cos\theta\cos\varphi & \sin\theta\cos\varphi \\ \sin\varphi\cos\psi\cos\theta + \sin\psi\cos\varphi & -\sin\psi\sin\psi\cos\theta + \cos\varphi\cos\psi & \sin\varphi\sin\theta \\ -\sin\theta\cos\psi & \sin\psi\cos\theta & \cos\theta \end{pmatrix}, \tag{16}$$

and P is a diagonal matrix consisting of the leading coefficients of relation (8) at $\lambda = 0$:

$$P = \begin{pmatrix} \alpha_0 & 0 & 0 \\ 0 & \beta_0 & 0 \\ 0 & 0 & \gamma_0 \end{pmatrix}, \quad (17)$$

where $\alpha_0 = \int_0^\infty \frac{\phi(S)\,dS}{a^2+s}$, $\beta_0 = \int_0^\infty \frac{\phi(S)\,dS}{b^2+s}$, $\gamma_0 = \int_0^\infty \frac{\phi(S)\,dS}{c^2+S}$, $\Phi(s) = \frac{abc}{\sqrt{(a^2+s)(b^2+s)(c^2+s)}}$.

The matrix J describes the velocity on the core surface caused by the rotation of the ellipsoid (core) as a whole:

$$J = \begin{pmatrix} 0 & -\dot\psi - \dot\varphi\cos\theta & \dot\varphi\sin\theta\cos\psi - \dot\theta\sin\psi \\ \dot\psi + \dot\varphi\cos\theta & 0 & -\dot\varphi\sin\theta\sin\psi - \dot\theta\cos\psi \\ -\dot\varphi\sin\theta\cos\psi + \dot\theta\sin\psi & \dot\psi\sin\theta\sin\psi + \dot\theta\cos\psi & 0 \end{pmatrix}. \quad (18)$$

The matrix T describes the external flow with vertical shear Γ and is given as

$$T = R^{-1}\begin{pmatrix} 0 & 0 & \Gamma \\ 0 & 0 & 0 \\ 0 & 0 & 0 \end{pmatrix} R. \quad (19)$$

Finally, the matrix D describes the deformation of the boundary of the ellipsoidal core:

$$D = \begin{pmatrix} \dot a/a & 0 & 0 \\ 0 & \dot b/b & 0 \\ 0 & 0 & \dot c/c \end{pmatrix}. \quad (20)$$

The matrix calculation results are as follows:

$$A = F(G + T - J - D) = \begin{pmatrix} a_{11} & a_{12} & a_{13} \\ a_{21} & a_{12} & a_{23} \\ a_{31} & a_{32} & a_{33} \end{pmatrix},$$

$$a_{11} = \frac{\Gamma a(\sin\varphi\sin\psi - \cos\varphi\cos\psi\cos\theta)\sin\theta\cos\psi - \dot a}{a^3},$$

$$a_{12} = \frac{-\beta_0\cos\theta + \dot\psi + \dot\varphi\cos\theta - \Gamma(\sin\psi\sin\psi - \cos\varphi\cos\psi\cos\theta)\sin\psi\sin\theta}{a^2},$$

$$a_{13} = \frac{\gamma_0\sin\psi\sin\theta - \dot\varphi\sin\theta\cos\psi + \dot\theta\sin\psi - \Gamma(\sin\varphi\sin\psi - \cos\varphi\cos\psi\cos\theta)\cos\theta}{a^2},$$

$$a_{21} = \frac{\alpha\cos\theta - \dot\varphi\cos\theta - \dot\psi + \Gamma(\sin\psi\cos\psi + \sin\psi\cos\psi\cos\theta)\sin\theta\cos\psi}{b^2},$$

$$a_{22} = \frac{-b\Gamma(\sin\varphi\cos\psi + \sin\psi\cos\varphi\cos\theta)\sin\psi\sin\theta - \dot b}{b^3}, \quad (21)$$

$$a_{23} = \frac{\gamma_0\sin\theta\cos\psi + \dot\varphi\sin\psi\sin\theta + \dot\theta\cos\psi - \Gamma(\sin\varphi\cos\psi + \sin\psi\cos\varphi\cos\theta)\cos\theta}{b^2},$$

$$a_{31} = \frac{-\alpha_0\sin\psi\sin\theta + \dot\varphi\sin\theta\cos\psi - \dot\theta\sin\psi - \Gamma\sin\theta\cos\varphi\cos\psi}{c^2},$$

$$a_{32} = \frac{-\beta_0\sin\theta\cos\psi - \dot\varphi\sin\psi\sin\theta - \dot\theta\cos\psi + \Gamma\sin\psi\sin^2\theta\cos\varphi}{c^2},$$

$$a_{33} = \frac{\frac{1}{4}\Gamma c(-\sin(\varphi - 2\theta) + \sin(\psi + 2\theta)) - \dot c}{c^3}.$$

For the purpose of meeting the kinematic condition (15), the matrix A should be antisymmetric, in particular:

$$a_{11} = 0, \quad a_{22} = 0, \quad a_{33} = 0,$$
$$a_{12} = -a_{21}, \quad a_{13} = -a_{31}, \quad a_{23} = -a_{32}. \quad (22)$$

By applying the relations of the matrix A elements (21) into condition (22) and taking the fact into account that $\varepsilon = \frac{a}{b}$ and $K = \frac{c}{\sqrt{ab}}$, we obtain the desired system of five differential equations, which completely

describes the vortex trends in the external baroclinic flow:

$$\begin{aligned}
\dot{\varepsilon} &= -\tau\sin\theta[\sin2\psi\sin\varphi - \cos\theta\cos2\psi\cos\varphi]\varepsilon,\\
\dot{K} &= \frac{3}{4}\tau\sin2\theta\cos\varphi K,\\
\dot{\varphi} &= \frac{1}{2}(\Omega_1+\Omega_2)+\frac{1}{2}(\Omega_1-\Omega_2)\cos2\psi+\tau\left(\frac{K^2}{\sin\theta}\right)\\
&\times\left[\cos\theta\left(\frac{\sin^2\psi}{\varepsilon^{-1}-K^2}+\frac{\cos^2\psi}{\varepsilon-K^2}\right)\sin\varphi\right.\\
&\left.-\frac{1}{2}\left(\frac{1}{\varepsilon^{-1}-K^2}-\frac{1}{\varepsilon-K^2}\right)\cos2\theta\sin2\psi\cos\varphi\right],\\
\dot{\theta} &= \frac{1}{2}(\Omega_2-\Omega_1)\sin\theta\sin2\psi\\
&+\tau\left(\left(\sin^2\theta-K^2\cos2\theta\left(\frac{\cos^2\psi}{\varepsilon^{-1}-K^2}+\frac{\sin^2\psi}{\varepsilon-K^2}\right)\right)\cos\varphi\right.\\
&\left.+\frac{K^2}{2}\left(\frac{1}{\varepsilon^{-1}-K^2}-\frac{1}{\varepsilon-K^2}\right)\cos\theta\sin2\psi\sin\varphi,\right.\\
\dot{\psi} &= \cos\theta\left[\Omega_3-\frac{1}{2}(\Omega_1+\Omega_2)-\frac{1}{2}(\Omega_1-\Omega_2)\cos2\psi\right]\\
&\times\frac{\tau}{\sin\theta}\left[\left[\left[K^2\cos^2\theta\left(\frac{\sin^2\psi}{\varepsilon^{-1}-K^2}+\frac{\cos^2\psi}{\varepsilon-K^2}\right)\right.\right.\right.\\
&\left.\left.\left.-\sin^2\theta\frac{\cos^2\psi-\varepsilon^2\sin^2\psi}{1-\varepsilon^2}\right]\sin\varphi\right.\\
&\left.-\frac{1}{2}\left[\left(\frac{K^2}{\varepsilon^{-1}-K^2}-\frac{K^2}{\varepsilon-K^2}\right)\cos2\theta\right.\right.\\
&\left.\left.+\frac{1+\varepsilon^2}{1-\varepsilon^2}\sin^2\theta\right]\cos\theta\sin2\psi\cos\varphi\right],
\end{aligned}\tag{23}$$

where $\tau=\Gamma/\sigma$ is the dimensionless shear parameter and $\Omega_1,\Omega_2,\Omega_3$ are the dimensionless angular rotation velocity of an ellipsoid (vortex core) around three semi-axes. They are set as follows [2, 6, 19]:

$$\begin{aligned}
\Omega_1 &= \frac{1}{2}K\int_0^\infty\frac{sds}{\sqrt{(\varepsilon+s)(\varepsilon^{-1}+s)^3(K^2+s)^3}},\\
\Omega_2 &= \frac{1}{2}K\int_0^\infty\frac{sds}{\sqrt{(\varepsilon+s)^3(\varepsilon^{-1}+s)(K^2+s)^3}},\\
\Omega_3 &= \frac{1}{2}K\int_0^\infty\frac{sds}{\sqrt{(\varepsilon+s)^3(\varepsilon^{-1}+s)^3(K^2+s)}}.
\end{aligned}\tag{24}$$

The derivatives in (23) are calculated with respect to the dimensionless time σt and are designated with a point above the corresponding symbol:

$$\dot{\vec{f}}=\frac{d\vec{f}}{d(\sigma t)},\tag{25}$$

where $\vec{f}=(\varepsilon(t),K(t),\varphi(t),\Theta(t),\psi(t))^T$ is the column (status state) vector of the left side of (14), which completely describes the vortex trend in the external flow with vertical shear. Equations (23) automatically take the conservation condition of a vortex core volume into account.

The system (23)–(24) is written in a dimensionless form to underline some general features. Relation (23) includes only one external parameter of the problem: the relative velocity shear $\tau=\Gamma/\sigma$. Other parameters are geometric: the vortex elongation $\varepsilon=\frac{a}{b}$, its flattening $K=\frac{c}{\sqrt{ab}}$, and three orientation angles changing over time. Hence, the vortex behavior depends on τ as a parameter, on the initial conditions at $\varepsilon(0),K(0)$, and the initial values of three orientation angles. In this case, the vortex behavior similarity condition requires the equality of all six corresponding parameters. For this reason, such vortices will behave identically regardless of actual physical dimensions and core vorticity. Integral characteristics of the vortices are also not important. However, the fact should be taken into account that the geostrophic approximation should be valid in any case.

Based on preliminary numerical study, among the geometric characteristics, the plane inclination of the main section to the horizontal plane is an important initial geometric characteristic of the vortex. Therefore, special attention should be paid to the angle θ among initial orientation angles considered as secondary. We took this feature into account. Finally, it is interesting that replacing Γ and σ in system (23) by $-\Gamma$ and $-\sigma$ turns a dimensionless time in an opposite direction, whereas this system remains unchanged. Hence, if a vortex develops according to some type, then a vortex with an opposite vorticity sign and an opposite shear will develop in an opposite direction over time. In other words, if it is possible for a vortex to elongate into a thread, then the reverse process is also possible for other vortices, such as "pulling" the thread into a compact vortex.

NUMERICAL MODELING

No mathematical representation is available for equation system (23) which would make it possible to noticeably simplify this system. Therefore, the only way to study (23) is the numerical method. The corresponding software was written using the MATLAB language and the ode23 function to carry out the numerical solution of (14). It is a numerical solution of the second and third orders with an adaptive time step to solve the system (14) by the Runge–Kutta method. The Runge-Kutta method implemented using ode23 simultaneously computes approximate solutions of the second and third accuracy orders at the current step. The difference between these solutions is used as the estimated local error. MATLAB checks whether the local error exceeds a user-specified or standard toler-

ance. This tolerance is specified via the RelTol (relative error) or AbsTol (absolute error) parameters. If the local error is too large (higher than the tolerance), the time step is reduced to improve the accuracy of the next step. If the error is small (much lower than the tolerance), the time step is increased to speed up the calculations. The relative tolerance RelTol = 10^{-6} was selected to implement the numerical solution (the code-writing code). When solving system (23), it is also necessary to specify the right side of (14) and initial values (conditions) of the status state vector $\vec{f}(t) = (\varepsilon(t), K(t), \varphi(t), \Theta(t), \psi(t))^T$. The problem is multidimensional and cannot be simplified analytically; therefore, to describe the vortex evolution in a flow, it is necessary to repeatedly solve numerically this system (23) by searching through initial problem conditions and parameters. Then, it is necessary to analyze the calculation results. The initial analysis of the results was also automated. The final conclusions were made by a human.

We selected the following conditions:

$$\begin{gathered}\varepsilon(0) \in \{1, 1.5, 2, 5, 10\},\\ K(0) \in \{0.1, 0.25, 0.5, 0.75, 1\},\\ \Theta(0) \in \left\{0, \frac{\pi}{6}, \frac{\pi}{3}, \frac{\pi}{2}, \frac{2\pi}{3}, \frac{5\pi}{6}, \pi\right\},\\ \varphi(0) = 0, \quad \psi(0) = 0.\end{gathered} \tag{26}$$

The vortex core evolution is highly dependent on the initial angle Θ and is slightly dependent on the initial angles φ and ψ; therefore, last two angles are initially equal to zero in the calculation series. The shear parameter τ is set from -0.5 to 0.5 with a step of 0.01. The parameter K is small for real ocean conditions, but it can reach values of about unit in the Arctic Ocean conditions. Hence, a series of $5 \times 5 \times 7 \times 101 = 17675$ calculations is reported in this paper. The system (14) solution for specific initial conditions of (17) represents the status state vector $\vec{f}(t)$ evolution over time. The set of solutions for different initial conditions (17) makes it possible to analyze the vortex trends in the external baroclinic flow with vertical shear.

VORTEX BEHAVIOR MODES IN A FLOW

When studying the ellipsoidal vortex evolution in a baroclinic flow, the most important issue is whether the vortex core remains a localized formation in terms of size, or whether the core is able to elongate indefinitely in any direction. In this respect, it is reasonable to compare the evolution modes of an ellipsoidal vortex under the influence of an equal-vortex barotropic flow with our problem. As is known, barotropic flows are characterized by three different vortex behavior modes [3, 4]: the core rotation mode, core nutational oscillation mode, and the mode of unlimited vortex elongation in a horizontal direction. In the first two modes, the vortex core remains as a localized formation (in other words, the vortex survives in the flow), although its size undergoes limited periodic oscillations. In the last mode, the flow destroys the vortex by elongating it indefinitely.

In a horizontal flow with vertical shear, the vortex behavior becomes more complicated. First of all, all three orientation angles and a length of all three semiaxes change over time. It is most convenient to observe such core evolution as the core projection onto a horizontal plane. In this case, if the projection size changes in time in a limited way, then the vortex is considered to survive in such flow and the mode is called the "survival mode." If the vortex projection is infinitely elongated in a horizontal direction, then such a vortex is destroyed by the background flow. The corresponding mode is called the "elongation (or destruction) mode." Possible intermediate options are discussed below.

The calculations obtained for the vortex behavior in a baroclinic background flow are as follows. In flows with vertical shear, a vortex is characterized by three behavior modes: (1) the vortex survival mode; (2) vortex elongation mode (or vortex destruction by a flow); and (3) the mode of a finite vortex lifetime with subsequent unlimited elongation.

In the survival mode, the vortex, remaining within a limited horizontal size, survives in the background flow for as long as desired. Such a vortex restrains the elongation effect of the background flow due to a considerable potential core vorticity. It is worth remembering that the studied core is vertically confined between two stationary horizontal planes, and the vertical size of the vortex therefore does not change in all modes. The survival mode occurs in two options: the core projection onto the horizontal plane rotates or oscillates around the vertical axis with simultaneous limited deformation of a horizontal size. The mode of all changes is quasi-periodic. In 3D space, the vortex core can rotate or oscillate around all directions. However, the condition that the vortex is confined between two horizontal planes leads to the fact that the main motion of the vortex shape is the core rotation or oscillation virtually around the vertical axis. Variations in principal directions along the conditionally horizontal axes lead to some swaying of the principal section $(x_1 O y_1)$ plane.

The unlimited elongation mode is characteristic for vortices with a relatively weak vorticity of the vortex core. In this case, elongation begins immediately at the initial time. The vortex turns around, is oriented along the flow, and is simultaneously elongated. In our terms, one of the conditionally horizontal axes is elongated, for example, the major axis a, with a simultaneous decrease in the conditionally vertical axis c to zero. In this mode, the second conditionally horizontal axis b retains a finite value. The final result of such elongation is vortex formation: thin in vertical, long

along the flow, and finite across the flow in the horizontal plane. In fact, such a formation can no longer be called a "vortex": all of its vortex features fade out as it is elongated. Most likely, this formation is similar to an element of the fine vertical ocean structure.

A new vortex behavior mode in a baroclinic flow can be described as follows: at the initial stage, the vortex develops as if it is in survival mode, in particular, it remains as a localized vortex formation for some time, its shape is limitedly deformed, rotated, or oscillated; then the rotation stops, the vortex is oriented along the flow and then is elongated indefinitely along the background flow. This elongation means the beginning of the end of the life of the vortex formation as a vortex. In this mode, the vortex lifetime is limited. This is called the "finite lifetime mode." It is fair to note that this mode was first described in [6]. However, other modes were not noted in this work.

A numerical experiment was carried out as follows. The dimensionless shear parameter $\tau = \Gamma/\sigma$ and initial problem conditions $\varepsilon(0), K(0), \varphi(0), \Theta(0), \psi(0)$ were selected. Then, all problem parameters were calculated according to system (23) using a dimensionless time interval of 10^4 units (corresponding, in order of magnitude, to a physical time from a few to 10 years). The result was analyzed in terms of $\varepsilon(t)$ and $K(t)$ trends. The calculation was repeated for other parameters: τ, $\varepsilon(0), K(0), \varphi(0), \Theta(0)$, and $\psi(0)$. The variation range of the dimensionless shear parameter $\tau = \Gamma/\sigma$ was tied to the $(-0.5; 0.5)$ segment. This range approximately corresponded to boundaries of the modes under study. As already noted, the vortex core behavior is highly dependent on the initial angle $\Theta(0)$ and is slightly dependent on the initial angles $\varphi(0)$ and $\psi(0)$; therefore, last two angles are initially equal to zero in the calculation series; the dependence of the solution types on these angles was not analyzed further. As a result, the set of main problem parameters on which the solution types depend is $\tau, \varepsilon(0), K(0)$, and $\Theta(0)$. In this set, τ is the dimensionless shear of the background flow, which does not change during the evolution of a particular vortex. This is an important external parameter of the problem. The second important dimensionless parameter describing geometric features of the vortex core is the initial vortex flattening parameter $K(0)$ which is consistent with the Burger number. It is convenient to depict the vortex behavior modes on the $(K(0), \tau)$ plane with fixed initial conditions for the remaining parameters $\varepsilon(0)$ and $\Theta(0)$.

Figures 2–8 show the behavior modes of the vortex core on the plane of the initial flattening parameter $K(0)$ and the shear parameter τ under different initial conditions $\varepsilon(0)$ and $\Theta(0)$. Red indicates the zone of vortex survival in the background flow, blue indicates the finite lifetime zone, and white indicates the zone of unlimited vortex elongation by the background flow. The unlimited elongation zone begins at the boundary of the blue zone and goes to plus and minus infinity along the τ axis.

The vortex behavior is very different when moving from the red zone to the blue one. Figures 9–11 show the evolution of vortex parameters in three zones.

As we can see, the vortex retains its relative shape for an infinitely long time in the red zone $(\sigma t = 10000)$. In other two zones, for the same time, the vortex is elongated into a thread when viewed from the side and, therefore, is destroyed due to viscosity and diffusion effects that are not taken into account in our approach.

Figures 12–14 show the vortex core with a unit volume in a fixed coordinate system for three zones at different moments of dimensionless time σt.

According to this visualization, the core evolution varies greatly in different zones. In the red zone, the core mostly retains its shape. In the blue zone, the vortex, starting from a certain point of time, is elongated indefinitely horizontally along the flow, remaining in finite horizontal dimensions across the flow and decreasing indefinitely vertically. In the white zone, the elongation process begins immediately. The possible core rotation in the horizontal plane projection is of particular interest.

The core evolution in the red zone is considered with initial values of $\varepsilon(0) = 1.5, K(0) = 0.25, \theta(0) = \frac{\pi}{6}$, $\tau = -0.06$. With these initial data, the vortex rotates intensively, mainly preserving its relative geometric shape. Figure 15 shows the vortex core in space at different moments in time.

Perhaps the most intriguing question in this paper is related to conditions under which the vortex survives in the above-mentioned background flow. Figures 2–8 make it possible to roughly determine the range of a dimensionless flow shear $\tau = \Gamma/\sigma$ corresponding to the red zone for different initial conditions of vortex parameters. It is clear in terms of physical considerations that the red zone corresponds to small values of τ: strong vortices survive in flows with a weak shear. The maximum possible range for the red zone parameter τ, taken from our calculations, is

$$-0.25 < \tau < 0.25 \qquad (27)$$

and is shown in Fig. 2 with initial conditions $\varepsilon(0) = 1.0$ and $\theta(0) = 0$. Condition (27) can be considered as sufficient for vortex survival in a shear flow (12). This condition means that vortices will survive if the potential vorticity of their vortex core σ (vortex intensity) exceeds the background flow shear Γ by at least four times. For other initial $\varepsilon(0)$ and $\theta(0)$ conditions, the excess of vortex intensity σ over Γ should be even greater. The interpretation of Figs. 2–8 together with

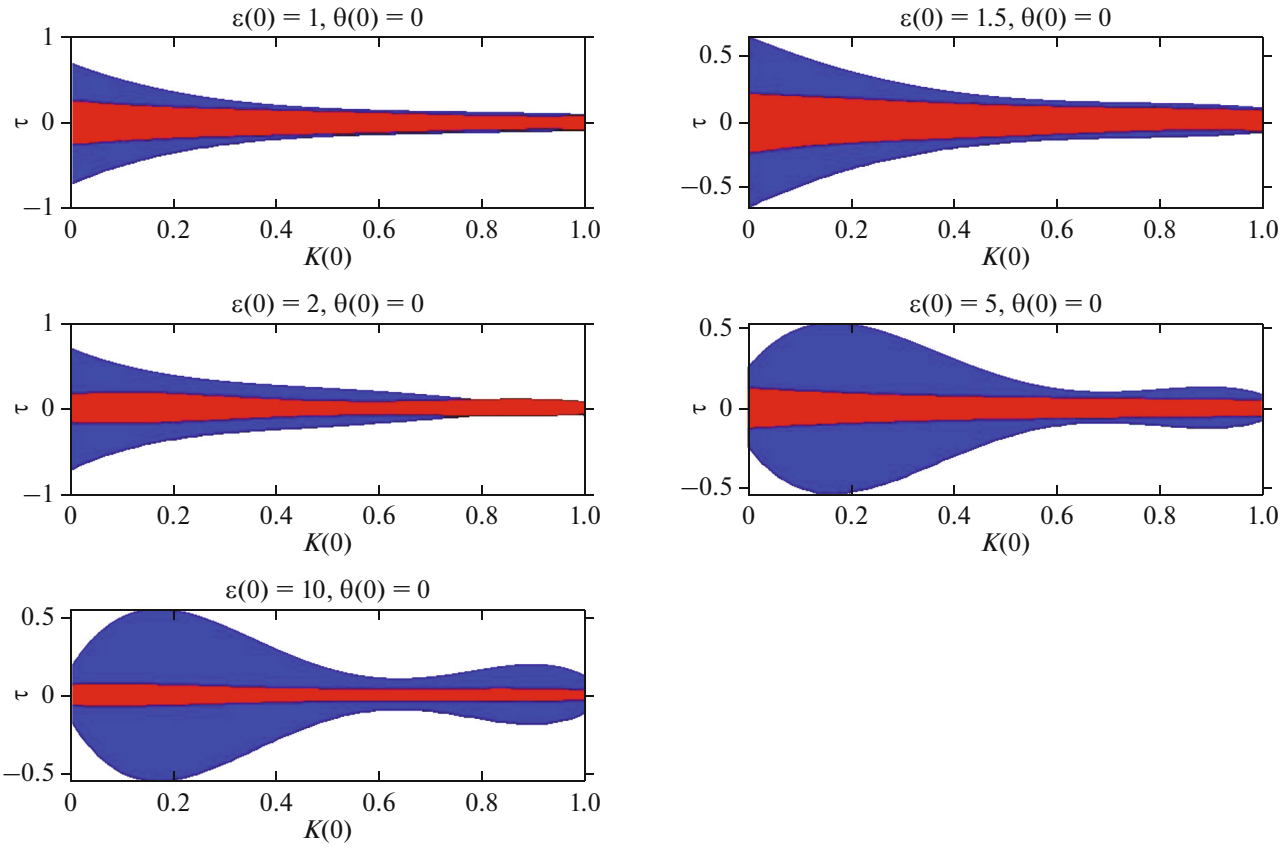

Fig. 2. Regions of the vortex core behavior modes in the plane of the initial flattening parameter $K(0)$ and the shear parameter τ: $K(0), \tau$ for initial values of $\varepsilon(0) \in \{1, 1.5, 2, 5, 10\}$ and $\Theta(0) = 0$. The red zone is the survival zone, the blue zone is the finite lifetime zone, and the white zone is the unlimited elongation zone. For convenience purposes, the initial values of $\varepsilon(0)$ and $\Theta(0)$ are shown above the picture in each drawing.

the necessary condition for vortex survival (27) makes it possible to conclude that only strong vortices with potential vorticity $|\sigma|$ considerably exceeding the background velocity shear $|\Gamma|$ survive in shear flows (12). Condition (27) yields the survival estimate

$$|\sigma| > 4|\Gamma|. \tag{28}$$

It should be noted that this estimate was obtained for special initial conditions. For other initial conditions, the inequality is larger and means that the vortex survival in the flow requires an even greater difference in $|\sigma|/|\Gamma|$ than indicated in (28).

We use relations (27) and (28) to estimate the minimum velocity shift $|\Gamma|$ necessary to provide an unlimited elongation of a vortex with a core vorticity σ. The geostrophic vortex intensity is estimated at $|\sigma| = (1\text{–}3)\times 10^{-5}\ \mathrm{s}^{-1}$. It is worth remembering that geostrophic conditions require a small Rossby number $\mathrm{Ro} = \left|\frac{\mathrm{rot}_z \vec{u}}{f}\right| \sim \left|\frac{\sigma}{f}\right| \ll 1$; therefore $|\sigma| = (1\text{–}3)\times 10^{-5}\ \mathrm{s}^{-1}$ corresponds to the real geostrophic vortex intensity. According to (27), the boundary between the red and blue zones is estimated by the shift parameter at $|\Gamma| = 0.25|\sigma| = 0.25(1\text{–}3)\times 10^{-5}\ \mathrm{s}^{-1} = (0.25\text{–}0.75)\times 10^{-5}\ \mathrm{s}^{-1} \sim 0.5\times 10^{-5}\ \mathrm{s}^{-1}$ corresponding to the velocity difference $0.5\ \frac{\mathrm{cm}}{\mathrm{s}}$ at 1 km in the vertical direction. This is a very moderate vertical velocity shift.

According to these estimates, almost all vortices should be destroyed by such flows, including calm zones with large-scale ocean circulation. However, in reality, vortices exist over a large area of the World Ocean. It should be noted that the given example idealizes the strong impact of the shear flow on mesoscale vortices, because the ocean along the vertical, together with the background flow, was considered to be infinite in our model. The finite vertical size of the background flow undoubtedly reduces the flow effect on the vortex. However, the qualitative conclusion that a flow with a noticeable vertical shear considerably affects the vortex survival in such flows remains valid. In addition, it becomes clear that a vertical shear

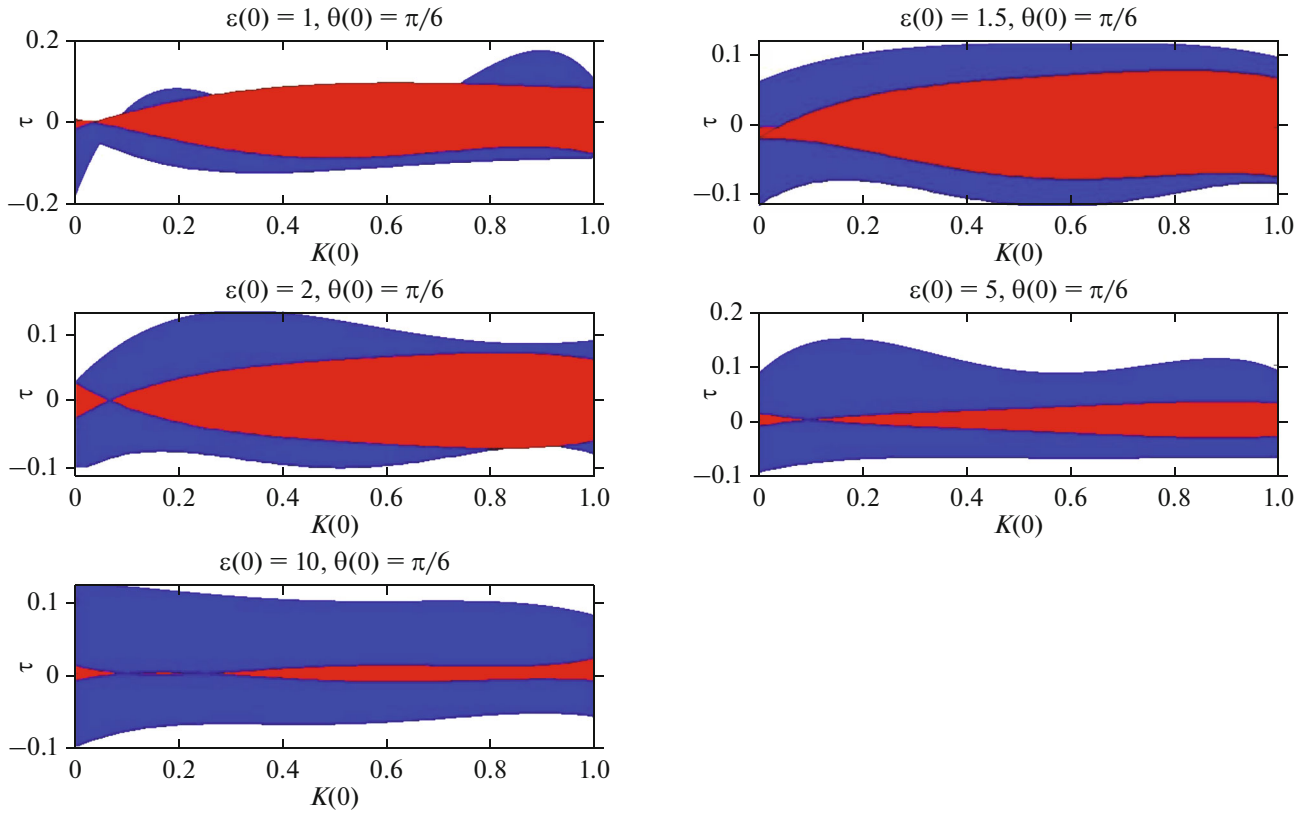

Fig. 3. Regions of the vortex core behavior modes in the plane of the initial flattening parameter $K(0)$ and the shear parameter τ $(K(0), \tau)$ for the initial values of $\varepsilon(0) \in \{1, 1.5, 2, 5, 10\}$ and $\Theta(0) = \frac{\pi}{6}$. The red zone is the survival zone, the blue zone is the finite lifetime zone, and the white zone is the elongation zone.

has a stronger effect on vortices than a horizontal shear. This feature is fully consistent with the suggestion that the baroclinic instability of the flow plays a more important role in mesoscale ocean trends than barotropic instability. It should also be expected that a flow with a strong vertical shear elongates vortices in a horizontal direction, turning vortex cores into elements with a fine vertical structure.

We can confirm this thesis based on [11], which studied the depth distribution of the number of vortices in the Gulf Stream region (Fig. 16 borrowed from this work).

As follows from Fig. 16, mesoscale and submesoscale vortices are completely absent in the layer from the surface to a depth of 1 km, where the estimated flow shear is the greatest. In our opinion, the vortices should be elongated indefinitely in this layer and subsequently be destroyed by the background flow. At a depth of 1–3 km, where the flow shear is noticeably less, the number of vortices increases considerably. We can suggest based on this fact that the local vortices resist the elongation effect of the background flow and survive more successfully in these conditions.

DISCUSSION AND INTERPRETATION

(1) This paper demonstrates three vortex behavior types in a baroclinic shear flow: the survival mode with an unlimited lifetime, the unlimited vortex elongation mode (or, in other words, a mode of vortex destruction by a flow), and, finally, the finite vortex lifetime mode. The last mode is interesting because the vortex evolution in the flow is similar to the survival mode for some time, but then the vortex stops, begins to be elongated, and goes into the destruction mode. The finite lifetime mode of vortices was first discussed in [6]. The other two modes were not considered in this work. A relation between dimensionless vortex lifetime σT and dimensionless vortex intensity σ/Γ in the form of a power law $\sigma T \sim (\sigma/\Gamma)^n$ was also proposed in [6]. An attempt to relate the vortex lifetime with its intensity in our problem for a wider σ/Γ range and other initial conditions using a similar relation was unsuccessful. This is indicative of more complicated relationships in the vortex–flow system.

(2) It is interesting to compare the vortex behavior in barotropic and baroclinic equal-vortex flows. The problem of a vortex in a barotropic flow was consid-

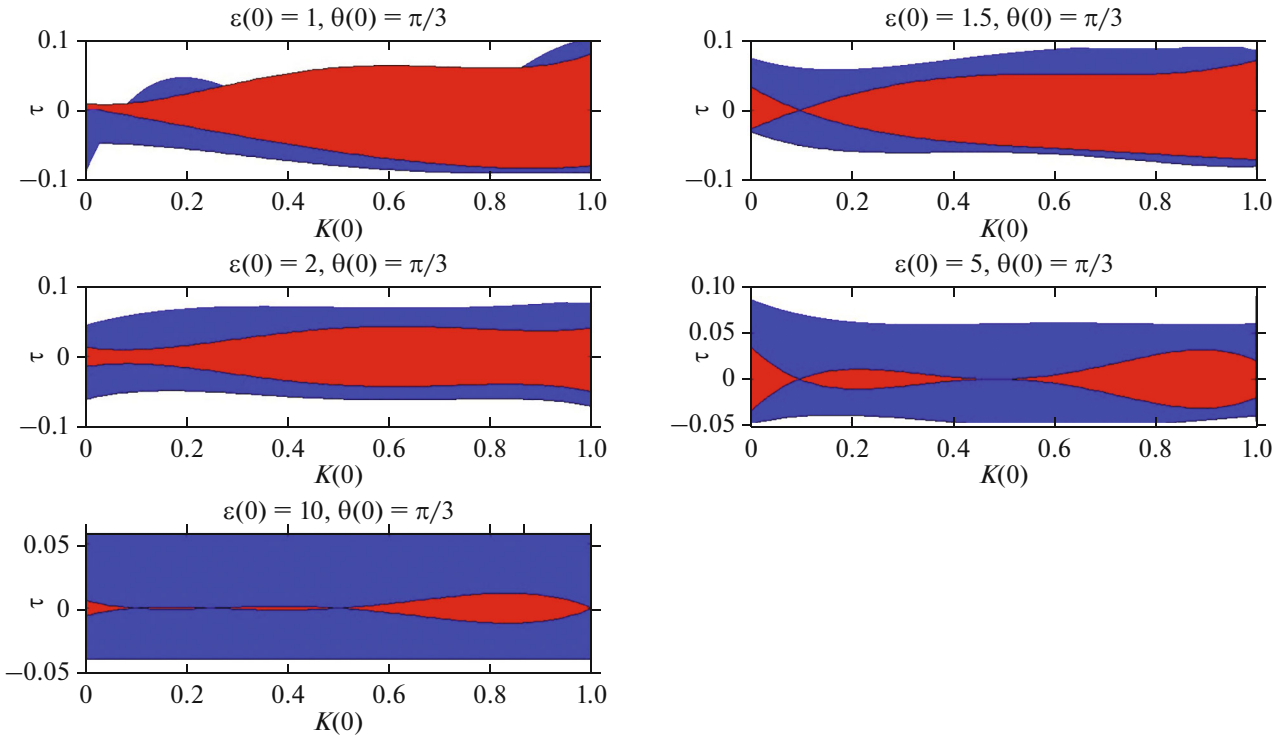

Fig. 4. Regions of the vortex core behavior modes in the plane of the initial flattening parameter $K(0)$ and the shear parameter τ $(K(0), \tau)$ for the initial values of $\varepsilon(0) \in \{1, 1.5, 2, 5, 10\}$ and $\Theta(0) = \frac{\pi}{3}$. The red zone is the survival zone, the blue zone is the finite lifetime zone, and the white zone is the elongation zone.

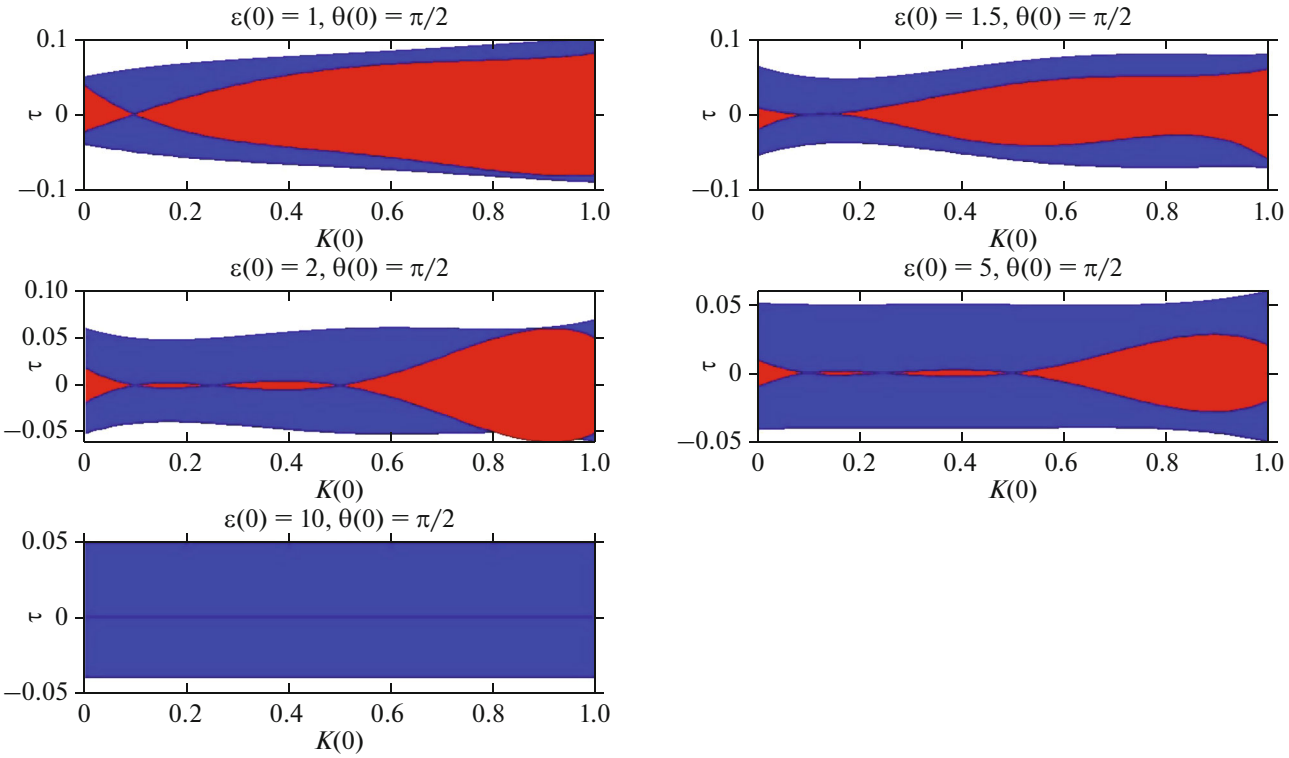

Fig. 5. Regions of the vortex core behavior modes in the plane of the initial flattening parameter $K(0)$ and the shear parameter τ $(K(0), \tau)$ for the initial values of $\varepsilon(0) \in \{1, 1.5, 2, 5, 10\}$ and $\Theta(0) = \frac{\pi}{2}$. The red zone is the survival zone, the blue zone is the finite lifetime zone, and the white zone is the elongation zone.

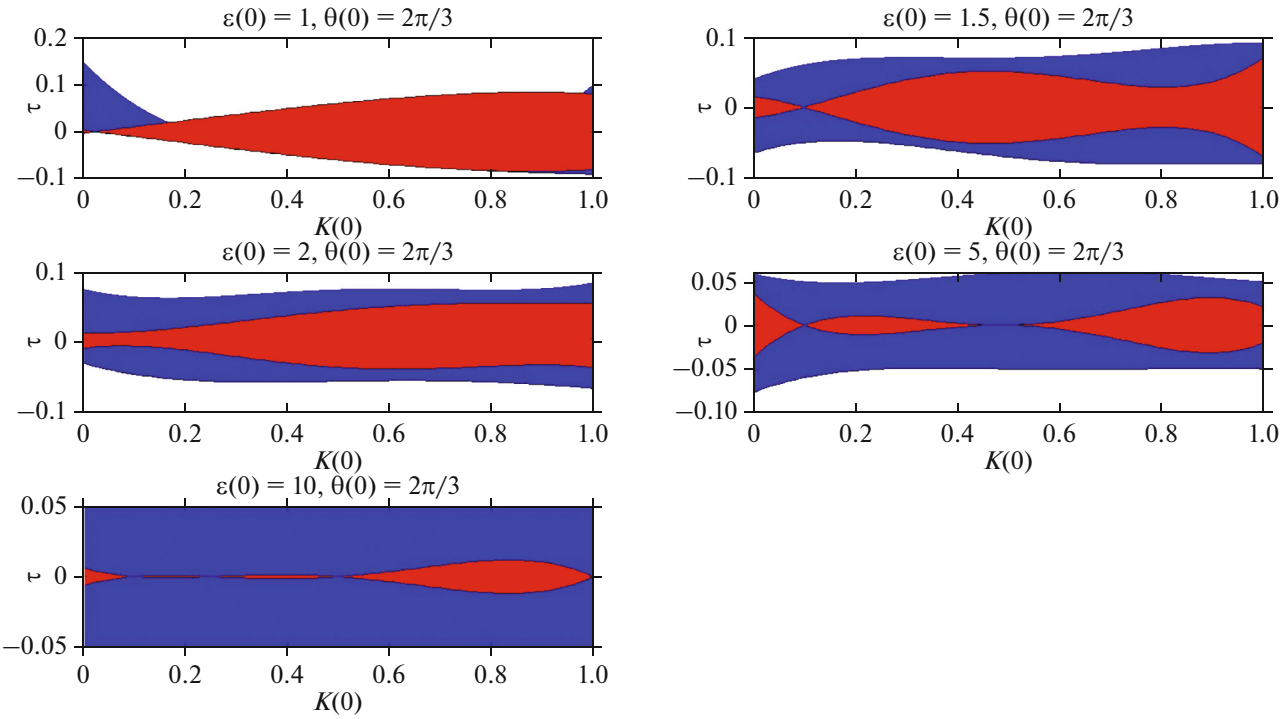

Fig. 6. Regions of the vortex core behavior modes in the plane of the initial flattening parameter $K(0)$ and the shear parameter τ $(K(0), \tau)$ for the initial values of $\varepsilon(0) \in \{1, 1.5, 2, 5, 10\}$ and $\Theta(0) = \frac{2\pi}{3}$. The red zone is the survival zone, the blue zone is the finite lifetime zone, and the white zone is the elongation zone.

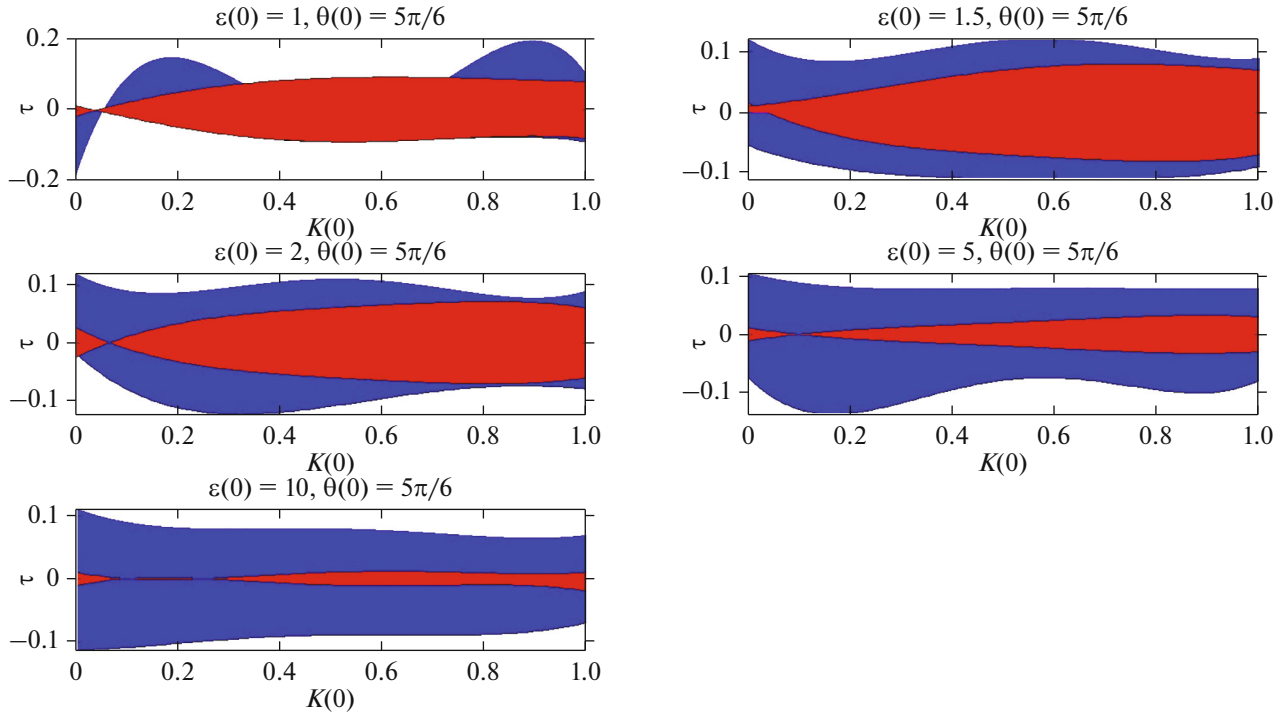

Fig. 7. Regions of the vortex core behavior modes in the plane of the initial flattening parameter $K(0)$ and the shear parameter τ $(K(0), \tau)$ for the initial values of $\varepsilon(0) \in \{1, 1.5, 2, 5, 10\}$ and $\Theta(0) = \frac{5\pi}{6}$. The red zone is the survival zone, the blue zone is the finite lifetime zone, and the white zone is the elongation zone.

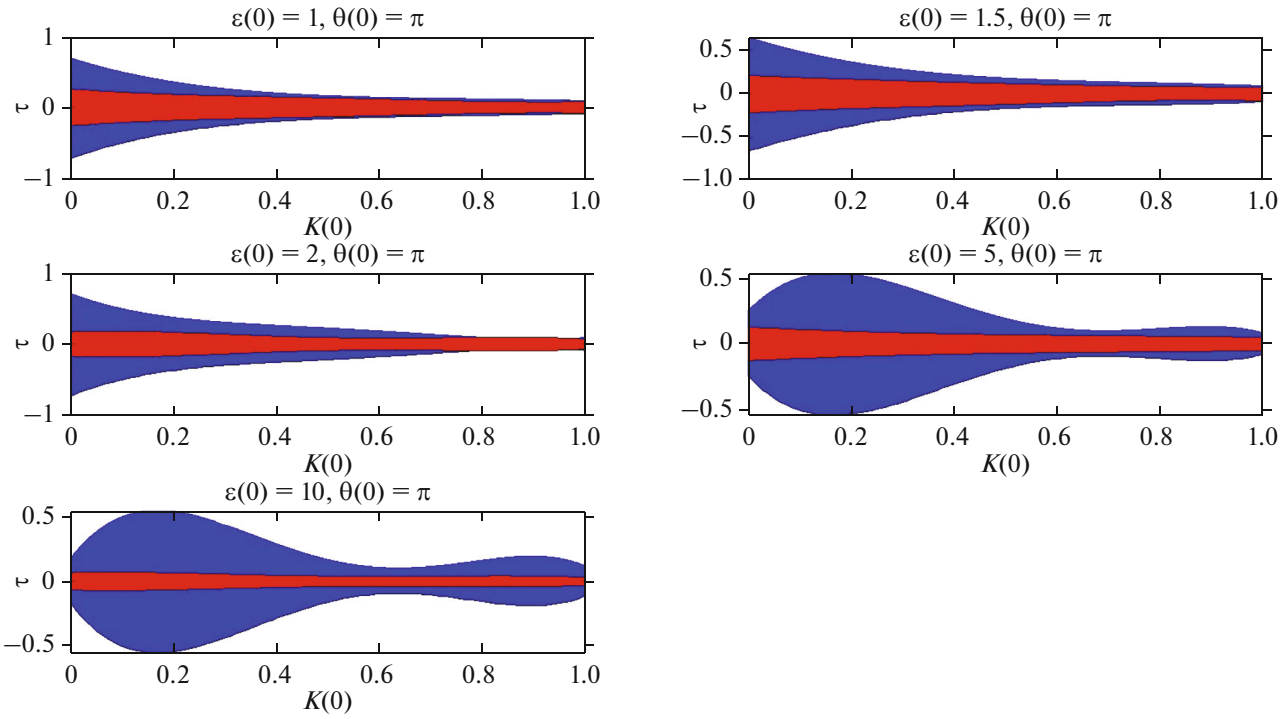

Fig. 8. Regions of the vortex core behavior modes in the plane of the initial flattening parameter $K(0)$ and the shear parameter τ $(K(0), \tau)$ for the initial values of $\varepsilon(0) \in \{1, 1.5, 2, 5, 10\}$ and $\Theta(0) = \pi$. The red zone is the survival zone, the blue zone is the finite lifetime zone, and the white zone is the elongation zone.

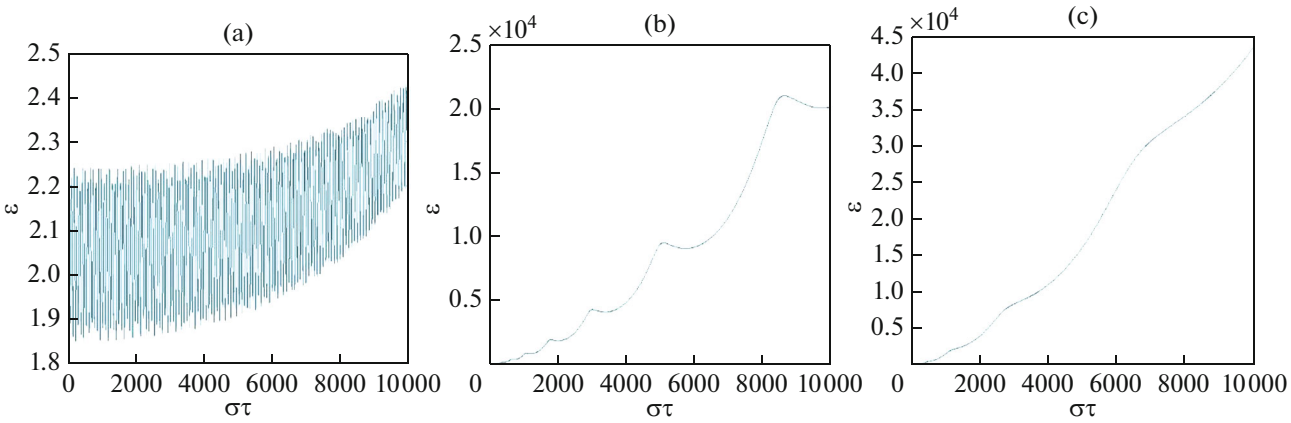

Fig. 9. The evolution of the vortex elongation parameter ε over dimensionless time σt in the (a) red, (b) blue, and (c) white zones with initial parameters $\varepsilon(0) = 2$, $K(0) = 0.5, \theta(0) = \frac{\pi}{3}$ and shear parameters (a) $\tau = -0.01$, (b) $\tau = 0.06$, and (c) $\tau = 0.1$.

ered most thoroughly in [3]: three types of vortex behavior were noted, two of which could be combined into one mode similar to the vortex survival in a baroclinic flow, and the remaining one was unlimited vortex elongation by the flow. Thus, a richer set of modes is observed in the baroclinic flow. This is characterized by the vortex finite lifetime mode, which is absent in the case of the barotropic background flow effect on the vortex. The vortex unlimited elongation patterns also differ in two flow types. In both cases, the elongation is horizontal. However, in the case of barotropic flows, in the horizontal direction perpendicular to the elongation direction, the size of the elongated vortex formation formally decreases to zero, whereas in the

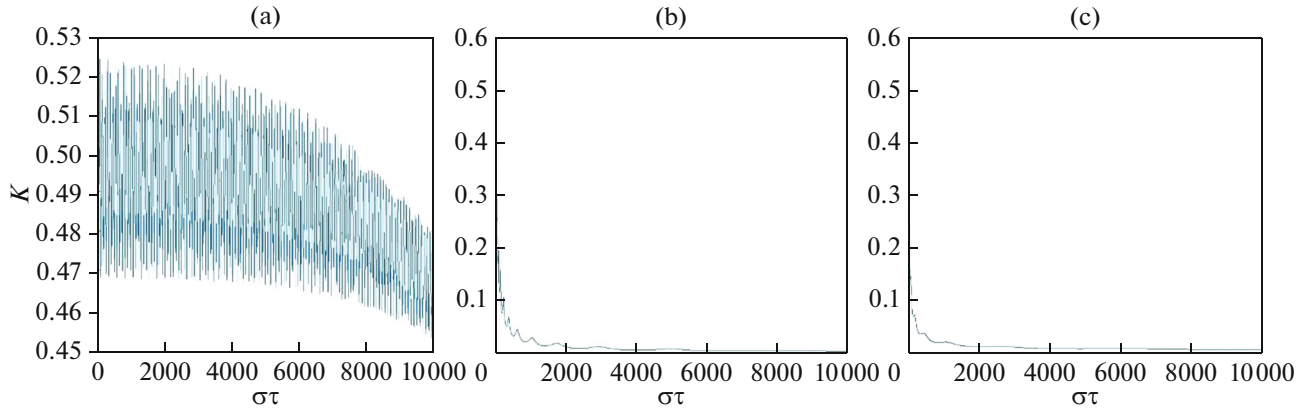

Fig. 10. The evolution of the vortex elongation parameter K over dimensionless time σt in the (a) red, (b) blue, and (c) white zones with initial parameters $\varepsilon(0) = 2,\ K(0) = 0.5, \theta(0) = \frac{\pi}{3}$ and shear parameters (a) $\tau = -0.01$, (b) $\tau = 0.06$, and (c) $\tau = 0.1$.

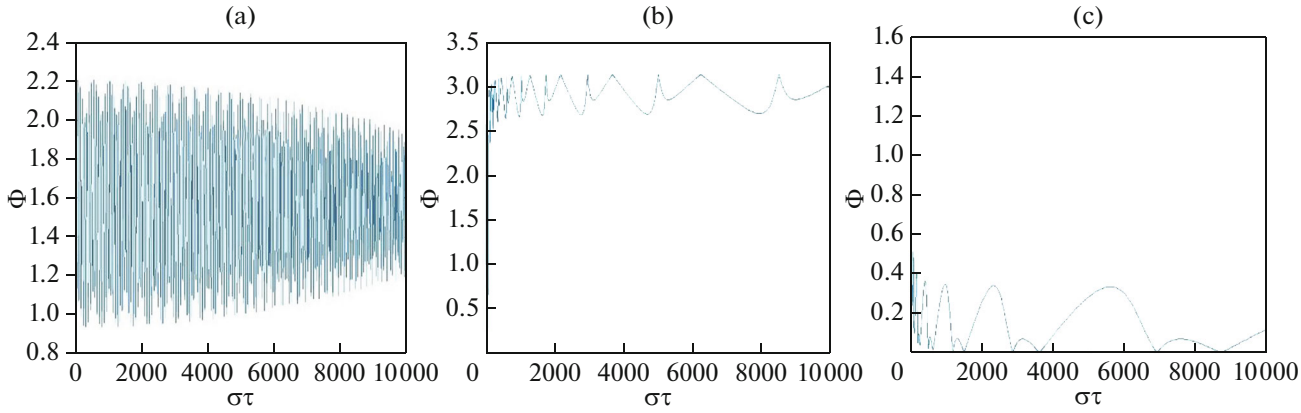

Fig. 11. The evolution of the vortex nutation angle θ over dimensionless time σt in the (a) red, (b) blue, and (c) white zones with initial parameters $\varepsilon(0) = 2, K(0) = 0.5, \theta(0) = \frac{\pi}{3}$ and shear parameters (a) $\tau = -0.01$, (b) $\tau = 0.06$, and (c) $\tau = 0.1$.

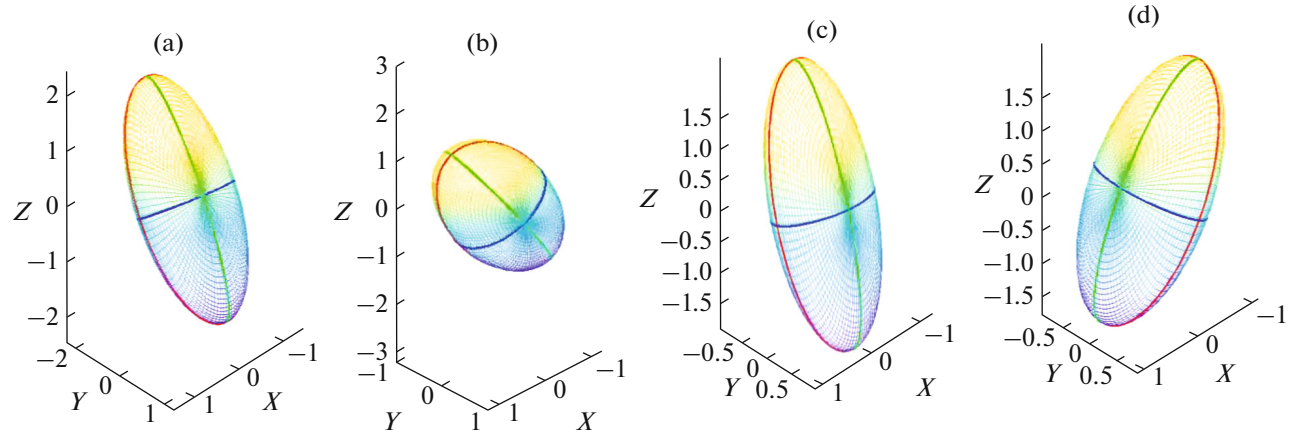

Fig. 12. The orientation and shape of the vortex core in the three-dimensional XYZ space for initial values $\varepsilon(0) = 2$, $K(0) = 0.5, \theta(0) = \frac{\pi}{3}$, and $\tau = -0.01$ in the red zone at time (a) $\sigma t = 0$, (b) $\sigma t = 100$, (c) $\sigma t = 1000$, and (d) $\sigma t = 10000$.

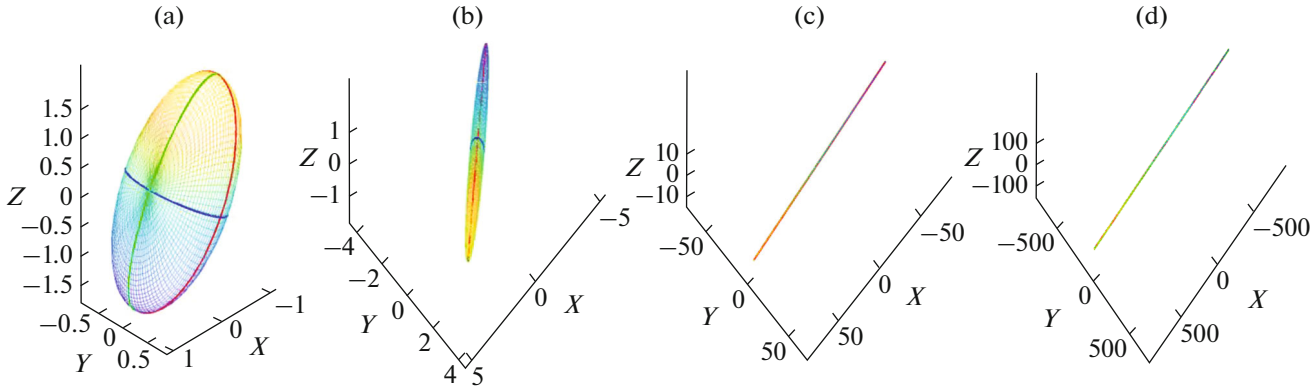

Fig. 13. The orientation and shape of the vortex core in the three-dimensional XYZ space for initial values $\varepsilon(0) = 2, K(0) = 0.5, \theta(0) = \frac{\pi}{3}$, and $\tau = 0.06$ in the blue zone at time (a) $\sigma t = 0$, (b) $\sigma t = 100$, (c) $\sigma t = 1000$, and (d) $\sigma t = 10000$.

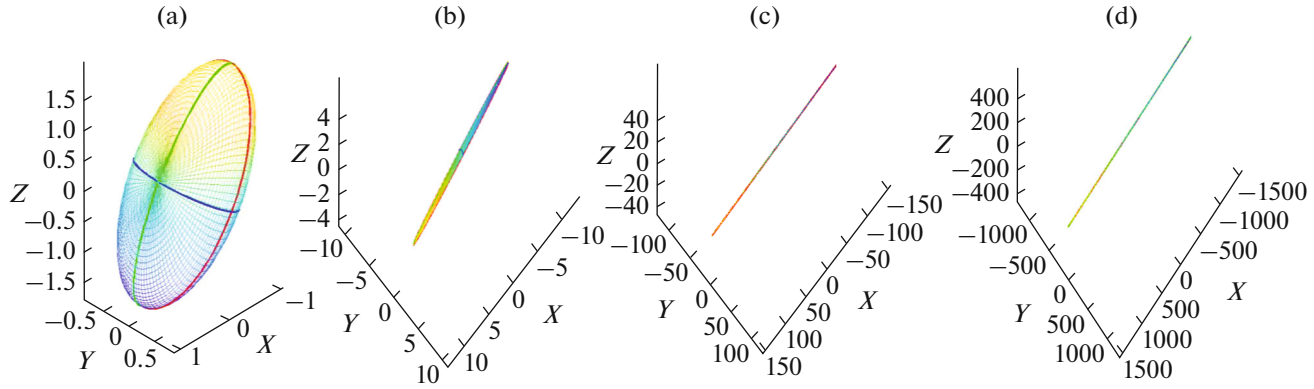

Fig. 14. The orientation and shape of the vortex core in the three-dimensional XYZ space for initial values $\varepsilon(0) = 2, K(0) = 0.5, \theta(0) = \frac{\pi}{3}$, and $\tau = 0.1$ in the white zone at time (a) $\sigma t = 0$, (b) $\sigma t = 100$, (c) $\sigma t = 1000$, and (d) $\sigma t = 10000$.

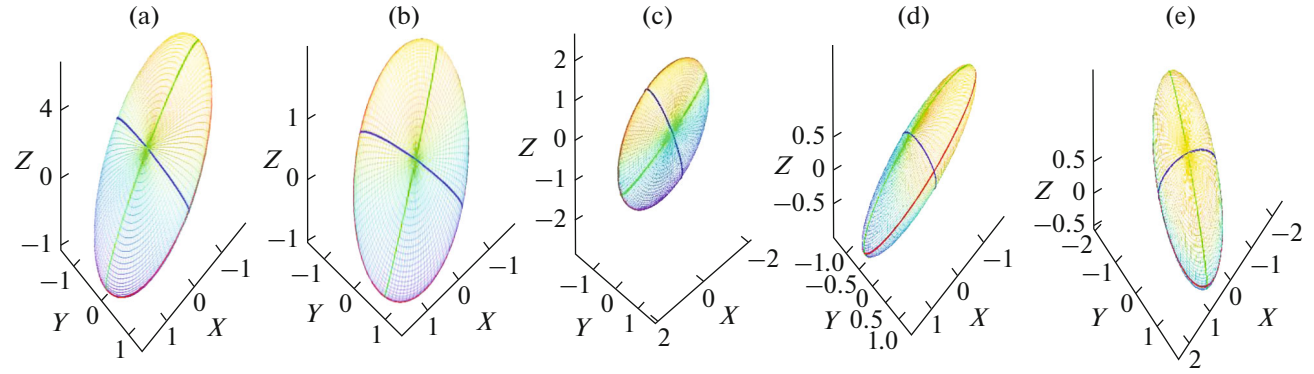

Fig. 15. The spatial orientation of the vortex core for initial values $\varepsilon(0) = 1.5, K(0) = 0.25, \theta(0) = \frac{\pi}{6}$, and $\tau = -0.06$ in the red zone at time (a) $\sigma t = 0$, (b) $\sigma t = 100$, (c) $\sigma t = 1000$, (d) $\sigma t = 10000$, and (e) $\sigma t = 100000$.

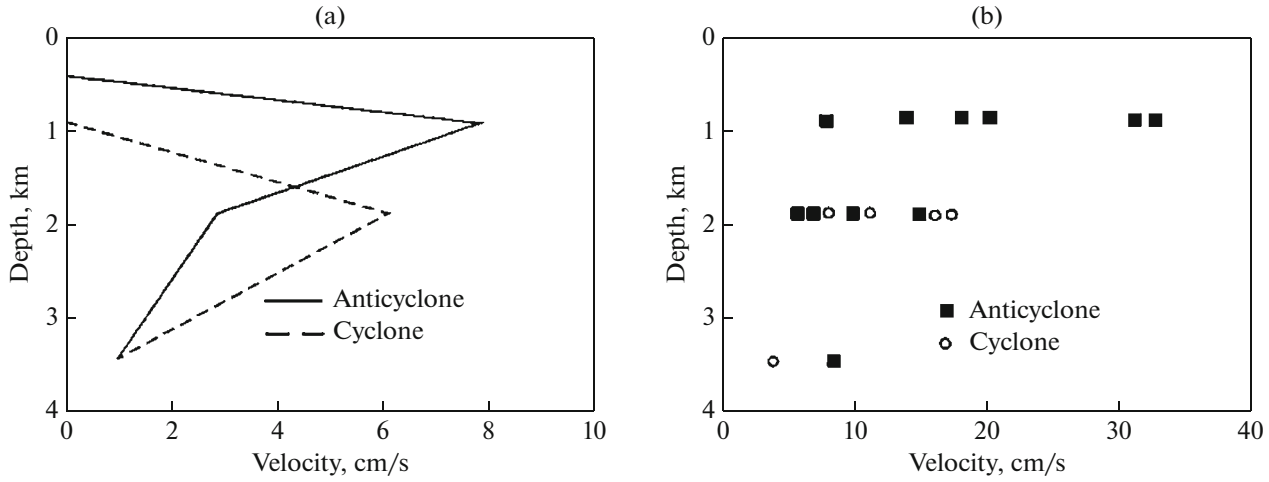

Fig. 16. (a) The depth distribution of the number of mesoscale vortices in the Gulf Stream region [11] and (b) maximum particle velocity in these vortices.

vertical direction, it remains finite. The vortex is transformed into a figure similar to a horizontally elongated band whose plane is vertical. When viewed from above, this formation resembles a vortex thread or a filament. Similar structures are observed in the ocean [4], although they are curved by background flows and are generally not straight segments. In the baroclinic flow studied in this paper the vortices are elongated differently. The vortex size increases without limits in the horizontal flow direction. In the horizontal direction perpendicular to the flow (in the flow plane), the vortex retains finite dimensions. In the vertical section, the core size formally decreases to zero. Hence, the final result of such transformation is a vortex formation as a horizontally elongated band. In contrast to the barotropic flow, the band plane is horizontal. When viewed from above, this formation also resembles a band. The geophysical interpretation of this transformation can be considered as the vortex transformation into a thin vertical ocean structure.

(3) Relation (27) together with Figs. 2–8 indicate that a considerable shear in a background velocity elongated the vortices, while a slight shear leaves them as compact vortex formations. This relation makes it possible to estimate the limiting shear that leads to changes in modes. According to the calculations, the limiting shear corresponds to a relatively negligible value of the shear parameter Γ, and, therefore, in theoretical terms, the vortex elongation should almost always be expected. However, this is not the case in natural conditions. Strong vortices survive in large numbers. Therefore, the critical shear value obtained from our theory is overestimated. What is the reason for this? We took the ocean and the flow as being infinite for the sake of mathematical simplicity. Following the gravity analogy, the pressure field in the vortex–flow system was mathematically analogous to the gravity potential in a star–interstellar dust system. The role of the vortex formation is played by a star, and that of the background flow is played by interstellar dust. The dust density is equivalent to a potential vorticity of the background flow, while the star density is equivalent to the potential vortex vorticity. In terms of mathematics, these problems are consistent. However, the fact should be taken into account that the motion is different in both cases. Obviously, if the volume of interstellar dust is limited, then the gravity effect of the dust on the star will decrease, just as limiting the flow size will lead to similar results in the problem related to the vortex behavior in the background flow. Limiting the vertical size of the background flow reduces the flow effect on the vortex. Thus, the shear intensity range $\tau = \Gamma/\sigma$ of the background flow should be reduced in inequality (27). This measure in turn will reduce the estimated critical velocity shear separating the vortex survival and destruction zones in the flow. In this case, an additional problem arises: how to take the limited vertical size of the flow in our problem into account, and what results will be obtained for the critical background velocity shear. This problem is a matter for further studies.

(4) Based on the fact that the unlimited vortex elongation mode exists, we can conclude that the reverse process is also possible in terms of mathematics: "contraction" of an elongated vortex structure into a compact vortex. In fact, replacing σ and Γ by $-\sigma$ and $-\Gamma$ does not lead to changes in equations (23) except one; the time flow will go in another direction. Therefore, it should be expected that under the same initial conditions, the evolution process of a new vortex in a new flow will develop in the opposite direction. Consequently, the phenomenon of unlimited vortex elongation in one case is accompanied by that of elongated vortex "contraction" into compact vortices in another case. The question arises: is this really correct and

where can such phenomenon be found in nature? We have known few cases of such behavior, while vortex threads observed in satellite images are a common phenomenon.

(5) It is known that long vortices are unstable. They disintegrate into a series of smaller vortices. Mathematical studies of this kind were carried out in the absence of background flows for Kirchhoff's flat vortices [8] and for volumetric ellipsoidal vortices in the presence of background flows [17]. The resistance of a vortex to disintegration into smaller vortices in the presence of nonuniform background flows has not been sufficiently studied, while baroclinic flows were not studied at all in this relation. These studies likely did not attract scientific interest. However, many vortex filaments (equivalent to long vortices) in nature do not disintegrate into smaller vortices. Hence, it can be concluded that background flows stabilize long vortices and prevent them from disintegrating. This issue is not completely clear. The influence of nonuniform background flows on the disintegration of long vortices into smaller varieties remains a matter of debate.

CONCLUSIONS

This paper solves the problem of vortex behavior in an external flow with vertical shear for a large number of problem parameters and initial conditions.

The evolution of the vortex core depends only on its initial geometric parameters, initial orientation angles and, most importantly, on the relative shear of the background flow (background flow shear/potential core vorticity). No integral characteristics of the vortex (for example, core integral vorticity and linear dimensions) affect its behavior. Such vortices, both large and small, behave in the same way. The vortex similarity conditions include one external dimensionless parameter of the problem (the relative shear of background velocity) and five geometric dimensionless parameters: elongation, flattening, and three orientation angles.

Three vortex behavior types on the plane of initial flattening parameters of the vortex core $K(0)$ and the dimensionless shear of the background flow τ were obtained as a result of the study of the vortex behavior in a shear flow: (1) a survival zone with infinite lifetime; (2) a finite lifetime zone; and (3) the elongation zone (or zone of vortex destruction by the flow). In the survival zone, the vortex maintains a finite size of its core, being in the oscillatory–rotation mode for an unlimited period. This is how intensive vortices behave in a flow with weak shear. In the finite lifetime zone the vortex initially behaves as it does in the survival zone; it is then oriented in a certain direction and then uniformly elongated by the flow. This zone corresponds to the finite vortex lifetime. However, the physical vortex lifetime varies over a wide range and can be either short or relatively long. This is how vortices with intermediate intensity behave. In the elongation zone, unlimited elongation begins from the initial moment of time corresponding to the destruction of the vortex by the flow from the very beginning of the vortex evolution in the external intensive flow. Such behavior is characteristic of weak vortices in the flow with strong shear.

Only intensive vortices with a high potential core vorticity can resist the effect of flow elongation on the vortex. A flow with strong shear elongates vortices in the horizontal direction, turning vortex cores into elements of the fine vertical structure. Theoretically, the reverse process is also possible, that is, the accumulation of vortex formation with a finite horizontal size from a horizontally long thin vertical structure.

FUNDING

The work was carried out under the state assignment of the Shirshov Institute of Oceanology, Russian Academy of Sciences (project no. FMWE-2024-0016, theoretical part of the work and analysis of the results obtained), and was supported by the Russian Science Foundation (grant no. 25-17-00021, numerical modeling).

ETHICS APPROVAL AND CONSENT TO PARTICIPATE

This work does not contain any studies involving human and animal subjects.

CONFLICT OF INTEREST

The authors of this work declare that they have no conflicts of interest.

REFERENCES

1. D. N. Elkin, A. G. Zatsepin, and D. R. Shvartsman, "Preliminary results of laboratory investigations of the evolution of non-frontal eddies in a two-layered rotating fluid," Okeanol. Issled. **51** (1), 5–35 (2023).
2. V. V. Zhmur, *Mesoscale Eddies in the Ocean* (GEOS, Moscow, 2011) [in Russian].
3. V. V. Zhmur, T. V. Belonenko, E. V. Novoselova, and B. P. Suetin, "Conditions for transformation of a mesoscale vortex into a submesoscale vortex filament when the vortex is stretched by an inhomogeneous barotropic flow," Oceanology **63** (2), 174–183 (2023). https://doi.org/10.1134/S0001437023020145
4. V. V. Zhmur, T. V. Belonenko, E. V. Novoselova, and B. P. Suetin, "Application to the World Ocean of the theory of transformation of a mesoscale vortex into a submesoscale vortex filament when the vortex is elongated by an inhomogeneous barotropic flow," Oceanology **63** (2), 184–194 (2023). https://doi.org/10.1134/S0001437023020157
5. V. V. Zhmur and K. K. Pankratov, "Dynamics of an ellipsoidal near-surface eddy in an inhomogeneous flow," Okeanologiya **29** (2), 205–211 (1989).

6. V. V. Zhmur and A. F. Shchepetkin, "Evolution of an ellipsoidal eddy in a stratified ocean in the f-plane approximation," Izv. Akad. Nauk SSSR, Fiz. Atmos. Okeana **27** (5), 492–503 (1991).
7. A. G. Zatsepin, V. I. Baranov, A. A. Kondrashov, A. O. Korzh, et al., "Submesoscale eddies at the caucasus Black Sea shelf and the mechanisms of their generation," Oceanology **51** (4), 554–567 (2011).
8. H. Lamb, *Hydrodynamics* (Cambridge Univ. Press, Cambridge, 1895).
9. A. N. Tikhonov and A. A. Samarskii, *Equations of Mathematical Physics*, 5th ed. (Nauka, Moscow, 1977) [in Russian].
10. S. A. Chaplygin, *Collected Works*, (Gostechnizdat, Moscow, 1948), **Vol. 2** [in Russian].
11. J. M. Bane, L. M. O'Keefe, and D. R. Watts, "Mesoscale eddies and submesoscale coherent vortices: their existence near and interaction with the Gulf Stream," in *Mesoscale/Synoptic Coherent Structures in Geophysical Turbulence*, Elsevier Oceanography Series (Elsevier, Amsterdam, 1989), **Vol. 50**, pp. 501–518.
12. S. A. Chaplygin, "On a pulsating cylindrical vortex," Trans. Phys. Sect. Imperial Moscow Soc. Friends of Natural Sciences **10** (1), 13–22 (1989).
13. D. G. Dritschel, J. N. Reinaud, and W. J. McKiver, "The quasi-geostrophic ellipsoidal vortex model," J. Fluid Mech. **505**, 201–223 (2004).
14. S. Kida, "Motion of an elliptic vortex in uniform shear flow," J. Phys. Soc. Jpn. **50** (10), 3517–3520 (1981).
15. G. Kirchhoff, *Vorlesungen über mathematische Physik: Mechanik* (Teubner, Leipzig, 1876).
16. W. J. McKiver and D. G. Dritschel, "The motion of a fluid ellipsoid in a general linear background flow," J. Fluid Mech. **474**, 147–173 (2003). https://doi.org/10.1017/S0022112002002859
17. W. J. McKiver and D. G. Dritschel, "The stability of a quasi-geostrophic ellipsoidal vortex in a background shear flow," J. Fluid Mech. **560**, 1–17 (2006).
18. W. J. McKiver and G. G. Dritschel, "Balanced solutions for an ellipsoidal vortex in a rotating stratified flow," J. Fluid Mech. **802**, 333–358 (2016). https://doi.org/10.1017/jfm.2016.462
19. S. P. Meacham, K. K. Pankratov, A. F. Shchepetkin, and V. V. Zhmur, "The interaction of ellipsoidal vortices with background shear flows in a stratified fluid," Dyn. Atmos. Oceans **21** (2–3), 167–212 (1994). https://doi.org/10.1016/0377-0265(94)90008-6
20. L. M. Polvani and G. R. Flierl, "Generalized Kirchhoff vortices," Phys. Fluids **29**, 2376–2379 (1986). https://doi.org/10.1063/1.865530
21. V. V. Zhmur and K. K. Pankratov, "Dynamics of desingularized quasigeostrophic vortices," Phys. Fluids A **3** (5), 1464–1464 (1991). https://doi.org/10.1063/1.857998

Translated by E. Maslennikova